A Second Order Convergent Trial Method for free Boundary Problems in Three Dimensions

Monica Bugeanu, Helmut Harbrecht

Institute of Mathematics
University of Basel
CH - 4051 Basel
Switzerland

Preprint No. 2014-14
October 2014

www.math.unibas.ch

A second order convergent trial method for free boundary problems in three dimensions

Monica Bugeanu
Department for Mathematics and Computer Science
Rheinsprung 21, 4051 Basel, Switzerland
monica.bugeanu@unibas.ch

Helmut Harbrecht
Department for Mathematics and Computer Science
Rheinsprung 21, 4051 Basel, Switzerland
helmut.harbrecht@unibas.ch

September 26, 2014

Abstract

The present article is concerned with the solution of a generalized Bernoulli free boundary problem by means of a trial method. At the free boundary, we prescribe the Neumann boundary condition and update the free boundary with the help of the remaining Dirichlet boundary condition. An inexact Newton update is used which results in a second order convergent iterative method. Numerical examples show the feasibility of the present approach.

Keywords: Free boundary problem; trial method; second order convergence.
2010 Mathematics Subject Classification: Primary 65N99; Secondary 35R35.

1 Introduction

The present article is devoted to the numerical solution of a free boundary problem of Bernoulli type by a second order convergent trial method. Let $S \subset \mathbb{R}^3$ denote a bounded and simply connected domain with boundary $\Sigma := \partial S$. Moreover, assume a second simply connected domain $T \subset \mathbb{R}^3$ with *free boundary* $\Gamma := \partial T$ which contains the fist domain, i.e. $\overline{S} \subset T$. The resulting annular domain is denoted by $\Omega := T \setminus \overline{S}$, see also Figure 1.1 for an illustration.

The free boundary problem now consists in finding a domain Ω and an associated function $u = u(\Omega) \in H^1(\Omega)$ such that the following overdetermined problem is satisfied:

$$\begin{aligned} -\Delta u &= f && \text{in } \Omega, \\ u &= g && \text{on } \Sigma, \\ -\frac{\partial u}{\partial \mathbf{n}} &= h, \quad u = 0 && \text{on } \Gamma. \end{aligned} \tag{1.1}$$

Figure 1.1: The interior boundary Σ and different approximations Γ_k to the sought free boundary Γ.

Throughout this article, we shall suppose that $g, h > 0$ and $f \geq 0$ are sufficiently smooth *functions* on $\mathbb{R}^n$ such that $u \in C^2(\overline{\Omega} \cap U)$ and U being a tubular neighbourhood of the free boundary Γ. We like to stress that the positivity of the Dirichlet data at the interior boundary implies (due to the maximum principle and the unique continuation property [23]) that u is positive on Ω and thus in fact $\partial u/\partial \mathbf{n} < 0$.

The trial method is a fixed point iteration for the sought free boundary. For the current free boundary, the solution of (1.1) is computed with one boundary condition at the free boundary and the other boundary condition is used for updating the free boundary. Trial methods for Bernoulli's free boundary problem based on a parametrization of the free boundary have been proposed in e.g. [1, 12, 35, 36]. Whereas, the level set method for representing the free boundary has been used in [4, 5, 26], enjoying the property of allowing topology changes.

An alternative approach for solving free boundary problems is shape optimization, see e.g. [8, 9, 20, 21, 24, 32] and the references therein, where in [15] a Newton method has been proposed for three dimensional free boundary problems. The different reformulations of Bernoulli type free boundary problems as shape optimization problems have been compared in [11]. We should finally also mention the pseudo-solid approach as a further solution technique for computing the solution of free boundary problems, see [22, 27, 37] for example.

The trial method which we propose in this article has been introduced and analyzed in [16]. Its convergence towards the optimal solution is locally quadratic. We will impose the Neumann boundary condition and update the free boundary according to the Dirichlet boundary condition. The particular update corresponds to an inexact Newton update and involves the so-called local shape derivative. The latter is a measure for the sensitivity when deforming the current computational domain by a given perturbation field. It is a well known quantity in shape calculus, see e.g. [8, 28, 31, 32] and the references therein.

We like to mention that a second order convergent trial method has already been proposed many years ago in [12, 36]. It is based on a Robin boundary value problem which involves the mean curvature of the free boundary. Unfortunately, if the free boundary becomes non-convex, this boundary

value problem is not elliptic any more and the trial method might diverge. This serious drawback is avoided by the trial method used in this article.

Throughout this article, we will not consider the interesting question of existence of optimal solutions. Instead, we will tacitly assume the existence of optimal domains, being *sufficiently regular* to apply shape calculus. For the existence of solutions to the generalized *exterior Bernoulli free boundary problem* (1.1), we refer the reader to e.g. [3], see also [12] for the related *interior* free boundary problem. Results concerning the geometric form of the solutions can be found in [2] and the references therein.

The outline of this article is as follows. Section 2 is dedicated to the trial method under consideration. The discretization of the free boundary is the topic of Section 3. Then, in Section 4, we discuss the efficient computation of the state by means of a fast wavelet based boundary element method. In Section 5, we perform numerical experiments to demonstrate the feasibility of the trial method. Finally, in Section 6, we state concluding remarks.

2 Trial method

2.1 Background and motivation

Throughout this article, we shall assume that the free boundary is of genus zero. Then, we can identify the domain Ω with a parametrization $\boldsymbol{\gamma} : \mathbb{S} \to \Gamma$ of its free boundary Γ. Here, $\mathbb{S} = \{\mathbf{x} \in \mathbb{R}^3 : \|\mathbf{x}\| = 1\}$ denotes the three-dimensional unit sphere.

The trial method for the solution of the free boundary problem (1.1) is a fixed point method for the unknown parametrization $\boldsymbol{\gamma}$ which reads as follows:

(1) Choose an initial guess Γ_0 of the free boundary and set $k = 0$.

(2a) Solve the boundary value problem

$$\begin{aligned} -\Delta u_k &= f \qquad \text{in } \Omega_k, \\ u_k &= g \qquad \text{on } \Sigma, \\ -\frac{\partial u_k}{\partial \mathbf{n}_k} &= h \qquad \text{on } \Gamma_k. \end{aligned} \tag{2.1}$$

(2b) Update the free boundary Γ_k by moving the old boundary into the normal direction $\mathbf{n}_k$:

$$\boldsymbol{\gamma}_{k+1} = \boldsymbol{\gamma}_k + \delta_k \mathbf{n}_k. \tag{2.2}$$

(3) Increase $k \mapsto k + 1$ and repeat step (2) until the process becomes stationary up to a specified accuracy.

The most common update function $\delta_k = \Psi(\boldsymbol{\gamma}_k) \in C^2(\mathbb{S})$ for (2.2) is determined in such a way that the desired homogeneous Dirichlet boundary condition is satisfied at the new boundary Γ_{k+1}, i.e.,

$$u_k \circ \boldsymbol{\gamma}_{k+1} \stackrel{!}{=} 0 \quad \text{on } \mathbb{S}, \tag{2.3}$$

where u_k is assumed to be smoothly extended into the exterior of Ω_k. The update function δ_k is found by linearizing $u_k \circ (\boldsymbol{\gamma}_k + \delta_k \mathbf{n}_k)$ with respect to the update function δ_k. This yields the equation

$$u_k \circ \boldsymbol{\gamma}_{k+1} \approx u_k \circ \boldsymbol{\gamma}_k + \left(\frac{\partial u_k}{\partial \mathbf{n}_k} \circ \boldsymbol{\gamma}_k \right) \delta_k. \tag{2.4}$$

Inserting the Neumann boundary condition $-\partial u_k / \partial \mathbf{n}_k = h$, we arrive at the following condition for the update $\delta_k^{(\mathrm{std})}$:

$$\delta_k^{(\mathrm{std})} = \Psi(\boldsymbol{\gamma}_k) := \frac{u_k \circ \boldsymbol{\gamma}_k}{h \circ \boldsymbol{\gamma}_k} : \mathbb{S} \to \mathbb{R} \tag{2.5}$$

This update rule has been used in e.g. [12, 26, 36], and yields a first order convergent trial method (see [36]). Notice that (2.5) is well defined since we assumed $h > 0$ to ensure the solvability of the free boundary problem.

Remark 2.1. The update $\delta_k^{(\mathrm{std})}$ from (2.5) is derived from the first order Taylor expansion (2.4). Instead, a second order Taylor expansion can also be used which would lead to a more stable trial method that, however, is also only first order convergent, cf. [16] for the details.

2.2 Speeding up the convergence

Clearly, the trial method converges if $\delta_k^{(\mathrm{std})} = \Psi(\boldsymbol{\gamma}_k) \to 0$ as $k \to \infty$. Hence, in order to arrive at a second order convergent trial method, we shall directly solve the equation

$$\Psi(\boldsymbol{\gamma}_k) \stackrel{!}{=} 0 \quad \text{on } \mathbb{S} \tag{2.6}$$

by a Newton-type method. In accordance with [16], the update which is implicitly given by

$$\delta_k^{(\mathrm{scd})} - \frac{\mathrm{d}u_k[\delta_k^{(\mathrm{scd})}] \circ \boldsymbol{\gamma}_k}{h \circ \boldsymbol{\gamma}_k} \stackrel{!}{=} \Psi(\boldsymbol{\gamma}_k). \tag{2.7}$$

corresponds to an inexact Newton method for the solution of (2.6). Herein, $\mathrm{d}u_k[\delta]$ is the local shape derivative in the direction δ which is given by (see [8, 29, 32] for example)

$$\begin{aligned} \Delta\, \mathrm{d}u_k[\delta] &= 0 && \text{in } \Omega_k, \\ \mathrm{d}u_k[\delta] &= 0 && \text{on } \Sigma, \\ \frac{\partial \mathrm{d}u_k[\delta]}{\partial \mathbf{n}_k} &= \delta \left[f - 2\mathcal{H}h - \frac{\partial h}{\partial \mathbf{n}_k} \right] + \mathrm{div}_\Gamma(\delta \nabla_\Gamma u_k) && \text{on } \Gamma_k. \end{aligned} \tag{2.8}$$

Note that the operator div_Γ denotes the surface divergence, the operator ∇_Γ denotes the surface gradient, and $\mathcal{H}$ denotes the mean curvature of the surface Γ.

The update $\delta_k^{(\mathrm{scd})}$ given by (2.7) does not coincide with the Newton update since we neglect the derivative of the denominator of the function Ψ from (2.5). This derivative is nevertheless zero if the field h is constant which holds for example in case of Bernoulli's original free boundary problem. Hence, in the latter situation, (2.7) coincides with the Newton update, as shown in the following

Theorem 2.2. Consider a constant field $h \equiv const.$ such that the update function (2.5) becomes

$$\Psi(\boldsymbol{\gamma}) := \frac{1}{h}(u \circ \boldsymbol{\gamma}).$$

Then, the derivative of Ψ in the direction $\delta\mathbf{n}$ is given by

$$\frac{\partial \Psi}{\partial(\delta\mathbf{n})}(\boldsymbol{\gamma}) = -\delta + \frac{1}{h}(\mathrm{d}u[\delta] \circ \boldsymbol{\gamma}).$$

Proof. Let the actual boundary Γ be described by $\boldsymbol{\gamma}$ and let the perturbed boundary be described by $\boldsymbol{\gamma}_\varepsilon = \boldsymbol{\gamma} + \varepsilon\delta\mathbf{n}$. Let u and u_ε denote the solutions to the underlying boundary value problems (2.1) relative to the domains Ω and Ω_ε , i.e.,

$$\begin{aligned} -\Delta u &= f \quad \text{in } \Omega, & -\Delta u_\varepsilon &= f \quad \text{in } \Omega_\varepsilon, \\ u &= g \quad \text{on } \Sigma, & u_\varepsilon &= g \quad \text{on } \Sigma, \\ -\frac{\partial u}{\partial \mathbf{n}} &= h \quad \text{on } \Gamma, & \frac{\partial u_\varepsilon}{\partial \mathbf{n}} &= h \quad \text{on } \Gamma_\varepsilon. \end{aligned}$$

Then, we have

$$\begin{aligned} \lim_{\varepsilon\to 0} \frac{\Psi(\boldsymbol{\gamma}_\varepsilon) - \Psi(\boldsymbol{\gamma})}{\varepsilon} &= \lim_{\varepsilon\to 0} \frac{1}{\varepsilon h}(u_\varepsilon \circ \boldsymbol{\gamma}_\varepsilon - u \circ \boldsymbol{\gamma}) \\ &= \lim_{\varepsilon\to 0} \frac{1}{\varepsilon h}\big\{u_\varepsilon \circ (\boldsymbol{\gamma}_\varepsilon - \boldsymbol{\gamma}) + (u_\varepsilon - u) \circ \boldsymbol{\gamma}\big\} \\ &= \frac{\delta}{h}\left(\frac{\partial u}{\partial \mathbf{n}} \circ \boldsymbol{\gamma}\right) + \frac{1}{h}(\mathrm{d}u[\delta] \circ \boldsymbol{\gamma}). \end{aligned}$$

By inserting the Neumann boundary condition $-\partial u/\partial\mathbf{n} = h$, we obtain the desired assertion. □

In case of a non-constant field h, the inexact Newton update computed via (2.7) approximates the exact Newton update with an absolute error that is of second order in the size of the exact Newton update, cf. [16]. The reason for this is that the enumerator becomes zero at the optimal free boundary. As a consequence, like the exact Newton method, the resulting inexact Newton method will converge (locally) quadratically to the sought free boundary, see, e.g., [13].

3 Discretization of the free boundary

3.1 Finite dimensional surface representation

We shall first introduce the spherical harmonics. For $n \in \mathbb{N}_0$ and $|m| \le n$, consider the Legendre polynomials

$$P_n(t) := \frac{1}{2^n n!}\Big(\frac{\mathrm{d}}{\mathrm{d}t}\Big)^n (t^2-1)^n, \quad t \in \mathbb{R},$$

and the associated Legendre functions

$$P_n^{|m|}(t) := (1-t^2)^{|m|/2}\Big(\frac{\mathrm{d}}{\mathrm{d}t}\Big)^{|m|} P_n(t), \quad t \in \mathbb{R}.$$

Then, the spherical harmonics $Y_n^m : \mathbb{S} \to \mathbb{R}$ are given by

$$Y_n^m(\widehat{\mathbf{x}}) := \sqrt{\frac{2n+1}{4\pi}\frac{(n-|m|)!}{(n+|m|)!}} P_n^{|m|}(\widehat{x}_3) \begin{cases} \mathrm{Re}\left((\widehat{x}_1 + i\widehat{x}_2)^m\right), & m \geq 0, \\ \mathrm{Im}\left((\widehat{x}_1 + i\widehat{x}_2)^m\right), & m < 0. \end{cases}$$

Since the spherical harmonics form an orthonormal basis of the Hilbert space of square-integrable functions defined on the unit sphere, each coordinate of the parametrization can be represented by a Fourier series which leads to the representation

$$\boldsymbol{\gamma}(\widehat{\mathbf{x}}) = \sum_{n=0}^{\infty} \sum_{m=-n}^{n} \mathbf{a}_{m,n} Y_n^m(\widehat{\mathbf{x}}), \quad \widehat{\mathbf{x}} \in \mathbb{S}, \tag{3.1}$$

with certain *vector valued* coefficients $\mathbf{a}_{m,n} \in \mathbb{R}^3$. Hence, it is reasonable to take the truncated series

$$\boldsymbol{\gamma}_N(\widehat{\mathbf{x}}) = \sum_{n=0}^{N} \sum_{m=-n}^{n} \mathbf{a}_{m,n} Y_n^m(\widehat{\mathbf{x}}), \quad \widehat{\mathbf{x}} \in \mathbb{S}, \tag{3.2}$$

as an approximation of $\boldsymbol{\gamma}$.

Notice that the representations (3.1) and (3.2), respectively, are not unique. Indeed, if $\Xi : \widehat{\Gamma} \to \widehat{\Gamma}$ denotes any smooth diffeomorphism, then the composed function $\boldsymbol{\gamma}_N \circ \Xi$ describes another parametrization of Γ. For the purpose of numerical computations, some parametrizations are preferable to others. We will specify this in Subsection 3.4. In order to discretize functions on the free boundary, we will use the parametrization (3.2) to map a subdivision of the parameter space $\widehat{\Gamma}$ to the actual boundary Γ. From this point of view it is obvious that, for numerical computations, a "nice" parametrization maps a uniform and shape regular mesh of the reference surface to a uniform and shape regular mesh on Γ. Therefore, we will introduce a suitable *mesh functional* $M(\Gamma)$ to monitor the quality of the mesh and apply from time to time a remeshing step to construct an appropriate re-parametrization of the free boundary.

3.2 Computing the updates

Let

$$\boldsymbol{\gamma}_N^{(k)}(\widehat{\mathbf{x}}) = \sum_{n=0}^{N} \sum_{m=-n}^{n} \mathbf{a}_{m,n}^{(k)} Y_n^m(\widehat{\mathbf{x}}), \quad \widehat{\mathbf{x}} \in \mathbb{S},$$

be the parametrization of the current free boundary Γ_k. To compute the new parametrization, we have to project the update $\delta_k \mathbf{n}_k$ computed by either (2.5) or (2.7) into the finite representation (3.2). Since the spherical harmonics are orthonormal, we find for the update

$$\begin{aligned} \boldsymbol{\gamma}_N^{(k+1)}(\widehat{\mathbf{x}}) &= \sum_{n=0}^{N} \sum_{m=-n}^{n} \mathbf{a}_{m,n}^{(k+1)} Y_n^m(\widehat{\mathbf{x}}) \\ &= \sum_{n=0}^{N} \sum_{m=-n}^{n} \left[\mathbf{a}_{m,n}^{(k)} + (\delta_k \mathbf{n}_k, Y_n^m)_{L^2(\mathbb{S})} \right] Y_n^m(\widehat{\mathbf{x}}), \quad \widehat{\mathbf{x}} \in \mathbb{S}. \end{aligned}$$

This means that the new coefficients $\{\mathbf{a}_{m,n}^{(k+1)}\}$ are obtained as the componentwise best approximation of $\boldsymbol{\gamma}_N^{(k)} + \delta_k \mathbf{n}_k$ with respect to the inner product in $L^2(\mathbb{S})$.

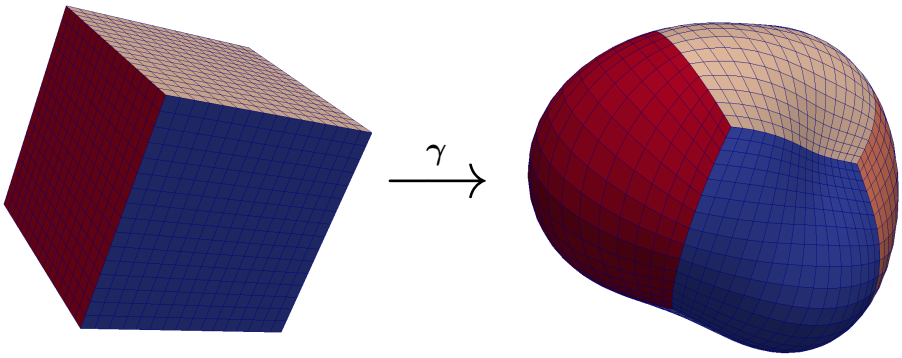

Figure 3.2: Parametric representation of Γ with quadrangular mesh on level 4.

3.3 Solving the second order update equation

The second order update $\delta_k^{(\mathrm{scd})}$ is given implicitly by the linear equation (2.7). To efficiently compute the sought update, we perform a Galerkin discretization of (2.7) by means of spherical harmonics: Seek $\delta_k = \sum_{n=1}^{N} \sum_{n=-m}^{m} b_n^m Y_n^m$ such that

$$(\mathbf{I} - \mathbf{A})\mathbf{b} = \mathbf{f},$$
$$\mathbf{A} = \left[\left(\tfrac{\mathrm{d}u_k[Y_n^m] \circ \boldsymbol{\gamma}_k}{h \circ \boldsymbol{\gamma}_k}, Y_{n'}^{m'} \right)_{L^2(\mathbb{S})} \right]_{(n,m),(n',m')}, \quad \mathbf{f} = \left[(\Psi(\boldsymbol{\gamma}_k), Y_n^m)_{L^2(\mathbb{S})} \right]_{(n,m)}, \tag{3.3}$$

where the vector $\mathbf{b} = [b_n^m]_{(n,m)}$ contains the unknown coefficients. This linear system of equations is solved by the GMRES method, introduced in [30]. In particular, in our numerical realization, we never assemble the system matrix but implemented the matrix-vector product.

3.4 Surface parametrization by quadrangular patches

We shall assume that the boundary manifolds Γ and Σ are given as parametric surfaces consisting of smooth patches. More precisely, let $\square := [0,1]^2$ denote the unit square. The manifold $\Gamma \cup \Sigma$ is partitioned into a finite number of *patches*

$$\Gamma \cup \Sigma = \bigcup_{i=1}^{M} \Gamma_i, \quad \Gamma_i = \boldsymbol{\kappa}_i(\square), \quad i = 1, 2, \ldots, M,$$

where each $\boldsymbol{\kappa}_i : \square \to \Gamma_i$ defines a diffeomorphism of $\square$ onto Γ_i. The intersection $\Gamma_i \cap \Gamma_{i'}$, $i \neq i'$, of two patches Γ_i and $\Gamma_{i'}$ is assumed to be either $\emptyset$, or a common edge, or a common vertex. A quadrangular mesh on the surface $\Gamma \cup \Sigma$ is then obtained by mapping a quadrangulation of $\square$ to $\Gamma \cup \Sigma$ via parametrization.

The construction of the parametric representation of the moving boundary Γ should be presented in more detail. Obviously, it suffices to construct such a parametrization of the reference manifold $\mathbb{S}$ which can be done as follows: The surface of the cube $[-0.5, 0.5]^3$ consists of six patches. Each point $\mathbf{x} \in \partial([-0.5, 0.5]^3)$ can be lifted onto the boundary Γ via the operation

$$\mathbf{y}(\mathbf{x}) = \boldsymbol{\gamma}\left(\frac{\mathbf{x}}{\|\mathbf{x}\|} \right) \in \Gamma. \tag{3.4}$$

In this manner, the surface Γ is subdivided into $M = 6$ patches. The parametric representations $\boldsymbol{\kappa}_i : \square \to \Gamma_i$ can easily be derived from (3.4). We refer to Fig. 3.2 for an illustration of the proposed parametric representation and mesh generation.

3.5 Improvement of the mesh quality

We shall specify the remeshing procedure as already used in [18]. A "nice" parametrization maps orthonormal tangents with respect to the unit cube onto orthogonal tangents of length $\approx |\Gamma|/6$ with respect to the boundary Γ. This means, that the first fundamental tensor of differential geometry, given by

$$\mathbf{K}_i(\mathbf{s}) = \left[\left\langle \frac{\partial \boldsymbol{\kappa}_i}{\partial x_j}(\mathbf{s}), \frac{\partial \boldsymbol{\kappa}_i}{\partial x_k}(\mathbf{s}) \right\rangle \right]_{j,k=1,2}, \quad \mathbf{s} = [s_1, s_2]^T \in \square,$$

satisfies $\mathbf{K}_i \approx |\Gamma|/6 \cdot \mathbf{I}$. Hence, the remeshing procedure will be based on the mesh functional

$$M(\Gamma) = \sum_{i=1}^{6} \int_{\square} \left\| \mathbf{K}_i(\mathbf{s}) - \frac{|\Gamma|}{6} \cdot \mathbf{I} \right\|_F^2 \mathrm{d}\mathbf{s}. \tag{3.5}$$

Based on the observation that the gradient of $M(\Gamma)$ with respect to the variable $\mathbf{s}$ is tangential, we may perform several gradient steps to minimize this mesh functional to increase the quality of the mesh.

4 Solving the state equation

4.1 Boundary integral equations

We will next discuss the numerical solution of (2.1) by means of a boundary element method. To that end, for sake of convenience, we skip the iteration index k in the present section. We first introduce a Newton potential N_f satisfying

$$-\Delta N_f = f \quad \text{in } \Omega. \tag{4.1}$$

The Newton potential is assumed to be explicitly known or to be computed with sufficiently high accuracy. The latter one has to be done only once in advance of the optimization process. The underlying domain needs to be large enough to ensure that Ω stays within it. However, it can be chosen fairly simple such that fast solvers are available.

The ansatz

$$u = N_f + v \tag{4.2}$$

reduces the state equation (2.1) to a Dirichlet problem for the Laplacian

$$\begin{aligned} \Delta v &= 0 && \text{in } \Omega, \\ v &= g - N_f && \text{on } \Sigma, \\ -\frac{\partial v}{\partial \mathbf{n}} &= h + \frac{\partial N_f}{\partial \mathbf{n}} && \text{on } \Gamma. \end{aligned} \tag{4.3}$$

We shall next introduce the single layer operator and the double layer operator with respect to the boundaries $\Phi, \Psi \in \{\Gamma, \Sigma\}$ by

$$(V_{\Phi\Psi}u)(\mathbf{x}) := \frac{1}{4\pi}\int_\Psi \frac{1}{\|\mathbf{x}-\mathbf{y}\|}u(\mathbf{y})\,\mathrm{d}\sigma_{\mathbf{y}}, \qquad \mathbf{x}\in\Phi,$$
$$(K_{\Phi\Psi}u)(\mathbf{x}) := \frac{1}{4\pi}\int_\Psi \frac{\langle \mathbf{x}-\mathbf{y}, \mathbf{n}_{\mathbf{y}}\rangle}{\|\mathbf{x}-\mathbf{y}\|^3}u(\mathbf{y})\,\mathrm{d}\sigma_{\mathbf{y}}, \quad \mathbf{x}\in\Phi.$$

Note that $V_{\Phi\Psi}$ denotes an operator of order -1 if $\Phi = \Psi$, i.e. $V_{\Phi\Phi} : H^{-1/2}(\Phi) \to H^{1/2}(\Phi)$, while it is an arbitrarily smoothing compact operator if $\Phi \neq \Psi$ since $\operatorname{dist}(\Gamma, \Sigma) > 0$. Likewise, if Σ, Γ are C^2-smooth, the double layer operator $K_{\Phi\Phi} : L^2(\Phi) \to L^2(\Phi)$ is compact while it is arbitrarily smoothing if $\Phi \neq \Psi$. We refer the reader to [14, 25, 33] for a detailed description of boundary integral equations.

The unknown boundary data of v are determined by

$$\begin{bmatrix} -V_{\Sigma\Sigma} & K_{\Sigma\Gamma} \\ -V_{\Gamma\Sigma} & \frac{1}{2}+K_{\Gamma\Gamma}\end{bmatrix}\begin{bmatrix}\frac{\partial v}{\partial \mathbf{n}}\big|_\Sigma \\ v|_\Gamma\end{bmatrix} = \begin{bmatrix} -(\frac{1}{2}+K_{\Sigma\Sigma}) & V_{\Sigma\Gamma} \\ -K_{\Gamma\Sigma} & V_{\Gamma\Gamma}\end{bmatrix}\begin{bmatrix}(g-N_f)\big|_\Sigma \\ -(h+\frac{\partial N_f}{\partial \mathbf{n}})\big|_\Gamma\end{bmatrix}. \tag{4.4}$$

The boundary integral operator on the left hand side of this coupled system of boundary integral equation is continuous and satisfies a Gårding inequality with respect to $H^{-1/2}(\Sigma)\times L^2(\Gamma)$. Since its injectivity follows from potential theory, this system of integral equations is uniquely solvable according to the Riesz-Schauder theory.

Likewise to (4.4), the unknown boundary data of the local shape derivative $\mathrm{d}u = \mathrm{d}u[\delta]$, defined in (2.8), are derived by the boundary integral equation

$$\begin{bmatrix} -V_{\Sigma\Sigma} & K_{\Sigma\Gamma} \\ -V_{\Gamma\Sigma} & \frac{1}{2}+K_{\Gamma\Gamma}\end{bmatrix}\begin{bmatrix}\frac{\partial\,\mathrm{d}u}{\partial \mathbf{n}}\big|_\Sigma \\ \mathrm{d}u|_\Gamma\end{bmatrix} = \begin{bmatrix} -(\frac{1}{2}+K_{\Sigma\Sigma}) & V_{\Sigma\Gamma} \\ -K_{\Gamma\Sigma} & V_{\Gamma\Gamma}\end{bmatrix}\begin{bmatrix}0 \\ \{\delta[f-2\mathcal{H}h-\frac{\partial h}{\partial \mathbf{n}}]+\operatorname{div}_\Gamma(\delta\nabla_\Gamma u)\}\big|_\Gamma\end{bmatrix}. \tag{4.5}$$

We would like to point out that the boundary integral operators are identical to those in (4.4) but the input data are different.

4.2 Wavelet based boundary element methods

We shall introduce the *wavelet Galerkin method* to solve the boundary integral equations (4.4) and (4.5). As crucial ingredient, we need a hierarchy of trial spaces $V_j \subset V_{j+1} \subset L^2(\partial\Omega)$. Such spaces can be constructed employing the parametric representation of the boundary.

We introduce a mesh of level j on the unit square by dyadic subdivisions of depth j into 4^j squares. On this mesh we consider piecewise bilinear nodal basis functions $\{\varphi^\square_{j,k} : k \in \triangle^\square_j\}$, where $\triangle^\square_j$ denotes a suitable index set satisfying $|\triangle^\square_j| = (2^j+1)^2$. We define a set of basis functions on the surface Γ via parametrization

$$\varphi^{\Gamma_i}_{j,k}(\mathbf{x}) := \begin{cases}\varphi^\square_{j,k}(\mathbf{s}), & \mathbf{x} = \boldsymbol{\gamma}_i(\mathbf{s}) \in \Gamma_i, \\ 0, & \text{elsewhere},\end{cases}$$

where $i = 1, 2, \ldots, M$. Glueing along the interfaces of the patches yields continuous bilinear ansatz functions $\{\varphi_{j,k}^{\partial\Omega} : k \in \triangle_j\}$, where $|\triangle_j| \sim M \cdot 4^j$. Obviously, the trial spaces

$$V_j := \operatorname{span}\{\varphi_{j,k}^{\partial\Omega} : k \in \triangle_j\} \subset H^1(\partial\Omega)$$

are nested with respect to j.

To obtain the Galerkin formulation of (4.4), we introduce for $\Phi, \Psi \in \{\Sigma, \Gamma\}$ the system matrices

$$\mathbf{V}_{\Phi\Psi} = \big[(V_{\Phi\Psi}\varphi_{j,k'}^{\Psi}, \varphi_{j,k}^{\Phi})_{L^2(\Phi)}\big]_{k,k'}, \quad \mathbf{K}_{\Phi\Psi} = \big[(K_{\Phi\Psi}\varphi_{j,k'}^{\Psi}, \varphi_{j,k}^{\Phi})_{L^2(\Phi)}\big]_{k,k'},$$

the mass matrices

$$\mathbf{G}_{\Phi} = \big[(\varphi_{j,k'}^{\Phi}, \varphi_{j,k}^{\Phi})_{L^2(\Phi)}\big]_{k,k'},$$

and the load vectors

$$\mathbf{f}_{\Sigma} = \big[(g - N_f, \varphi_{j,k}^{\Sigma})_{L^2(\Sigma)}\big]_k, \quad \mathbf{f}_{\Gamma} = \left[-\Big(h + \frac{\partial N_f}{\partial \mathbf{n}}, \varphi_{j,k}^{\Gamma}\Big)_{L^2(\Gamma)} \right]_k.$$

This leads to the boundary element method

$$\begin{bmatrix} -\mathbf{V}_{\Sigma\Sigma} & \mathbf{K}_{\Sigma\Gamma} \\ -\mathbf{V}_{\Gamma\Sigma} & \frac{1}{2}\mathbf{G}_{\Gamma} + \mathbf{K}_{\Gamma\Gamma} \end{bmatrix} \begin{bmatrix} \mathbf{v}_{\Sigma} \\ \mathbf{v}_{\Gamma} \end{bmatrix} = \begin{bmatrix} -(\frac{1}{2}\mathbf{G}_{\Sigma} + \mathbf{K}_{\Sigma\Sigma}) & \mathbf{V}_{\Sigma\Gamma} \\ -\mathbf{K}_{\Gamma\Sigma} & \mathbf{V}_{\Gamma\Gamma} \end{bmatrix} \begin{bmatrix} \mathbf{G}_{\Sigma}^{-1}\mathbf{f}_{\Sigma} \\ \mathbf{G}_{\Gamma}^{-1}\mathbf{f}_{\Gamma} \end{bmatrix} \tag{4.6}$$

which approximates the Dirichlet data $v|_{\Gamma} \approx \sum_k [\mathbf{v}_{\Gamma}]_k \, \varphi_{j,k}^{\Gamma}$ at the free boundary Γ and the Neumann data $(\partial v/\partial \mathbf{n})|_{\Gamma} \approx \sum_k [\mathbf{v}_{\Sigma}]_k \, \varphi_{j,k}^{\Sigma}$ at the interior boundary Σ. The sought Dirichlet and Neumann boundary data are computed in complete analogy where, by applying integration by parts, the load vector is given by

$$\mathbf{f}_{\Sigma} = \mathbf{0}, \quad \mathbf{f}_{\Gamma} = \left[\Big(\delta\Big[f - 2\mathcal{H}h - \frac{\partial h}{\partial \mathbf{n}}\Big], \varphi_{j,k}^{\Gamma}\Big)_{L^2(\Gamma)} - \big(\delta \nabla_{\Gamma} u, \nabla_{\Gamma}\varphi_{j,k}^{\Gamma}\big)_{L^2(\Gamma)} \right]_k.$$

Unfortunately, the system matrices $\mathbf{V}_{\Phi\Psi}$ and $\mathbf{K}_{\Phi\Psi}$ in (4.6) are densely populated. Moreover, the system matrix $\mathbf{V}_{\Phi\Phi}$ becomes more and more ill-conditioned when the level j of resolution increases. Thus, we end up with an at least quadratic complexity for computing the approximate solution of (4.3), i.e., the computational work scales at least like $\mathcal{O}(|\triangle_j|^2)$.

Instead of the single-scale basis $\{\varphi_{j,k}^{\partial\Omega} : k \in \triangle_j\}$, we will employ appropriate *biorthogonal spline wavelets* for the discretization of the boundary integral operators. Then, we obtain quasi-sparse system matrices having only $\mathcal{O}(|\triangle_j|)$ relevant matrix coefficients. Moreover, due to the norm equivalences of wavelet bases, an appropriate scaling of the bases yields a well-conditioned linear system of equations (cf. [7]). Applying the matrix compression strategy developed in [6] combined with an exponentially convergent hp-quadrature method [17], the wavelet Galerkin method produces the approximate solution of (4.3) within underlying discretization error accuracy in linear complexity.

5 Numerical results

5.1 First example

We will present numerical results which demonstrate the feasibility and efficiency of the second order convergent trial method that has been introduced in the previous sections. For our first example,

let the interior domain S be the L-shape

$$S = ([-0.5, 0.5] \times [-1, 1]^2) \setminus ([-0.5, 0.5] \times [0, 1]^2)$$

and consider the following free boundary problem: Find the free boundary Γ with associated solution $u = u(\Gamma)$ such that it holds

$$\begin{aligned} -\Delta u &= 1 && \text{in } \Omega, \\ u &= 1 && \text{on } \Sigma, \\ -\frac{\partial u}{\partial \mathbf{n}} &= h, \quad u = 0 && \text{on } \Gamma. \end{aligned}$$

The constant field h will vary in the example according to $h \equiv 1, 2, 3$. Notice that this example coincides with that from [10, 15], where first and second order shape optimization algorithms have been used for its solution.

In addition to the results for the second order convergent trial method, we shall also present results for the first order convergent trial method which uses the update (2.5), multiplied by the damping factor 1/2 to enforce convergence. It corresponds to the standard method and has been applied for sake of comparison.

The state equation is discretized on level 4 which yields about 4 500 piecewise bilinear boundary elements in accordance with Section 4. The particular Newton potential we use is analytically given by $N_f(x, y, z) = -(x^2+y^2+z^2)/6$. To approximate the free boundary, we use the first 100 spherical harmonics per coordinate of the parametrization, that is, harmonic polynomials up to order 10 can be represented exactly. In accordance with (3.2), this yields 300 design parameters in all. Furthermore, we apply 400 spherical harmonics for the Galerkin scheme (3.3) to compute the inexact Newton update.

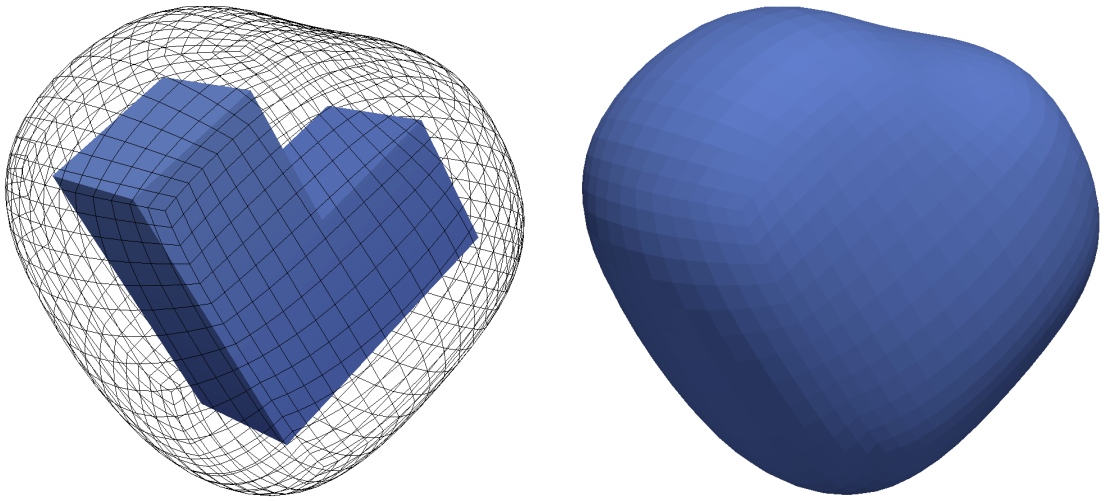

Figure 5.3: The free boundary of the first example in case of $h = 1$.

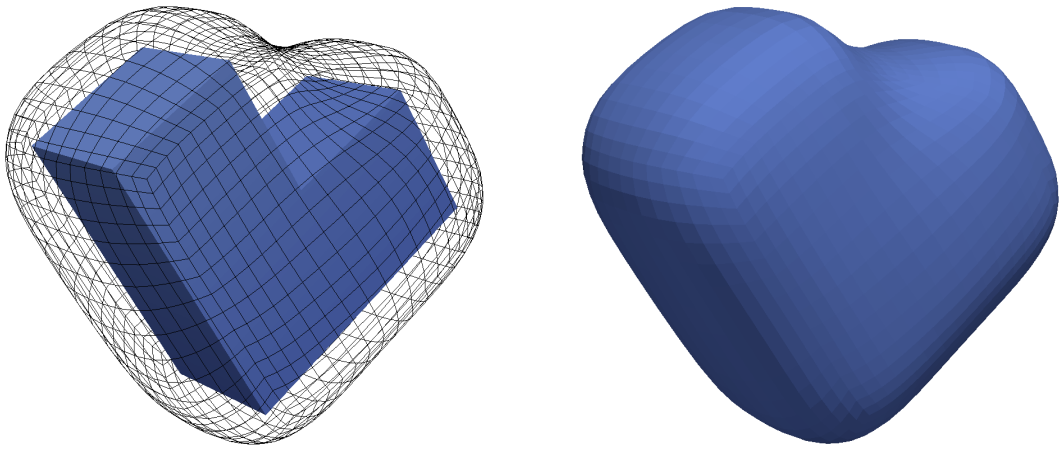

Figure 5.4: The free boundary of the first example in case of $h = 2$.

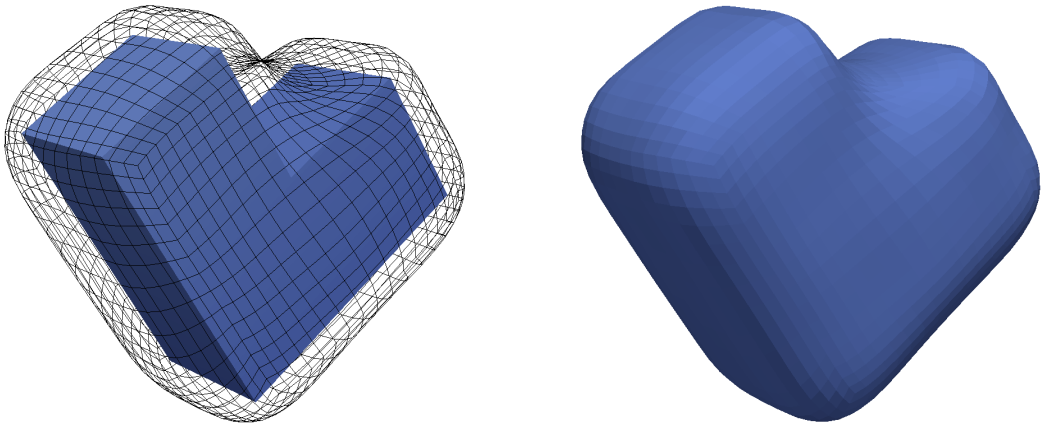

Figure 5.5: The free boundary of the first example in case of $h = 3$.

In all calculations, the sphere of radius 4 has been used as an initial guess for the free boundary. The computed free boundaries in case of $h \equiv 1, 2, 3$ are presented in Figures 5.3–5.5. Note that the mesh quality was always good during the iterative solution procedure for both trial methods such that a remeshing has never been necessary.

As seen in Figure 5.6, the first order convergent trial method converges very slowly while the second order convergent trial method needs at most 8 iterations to produce updates of the free boundary whose norm is always less than 10^{-3}. For the latter one, there are required in addition 8–10 iterations of the GMRES method per step to solve the update equation (2.7). This means that at most 10 times the local shape derivative (2.8) has to be determined. Nevertheless, their

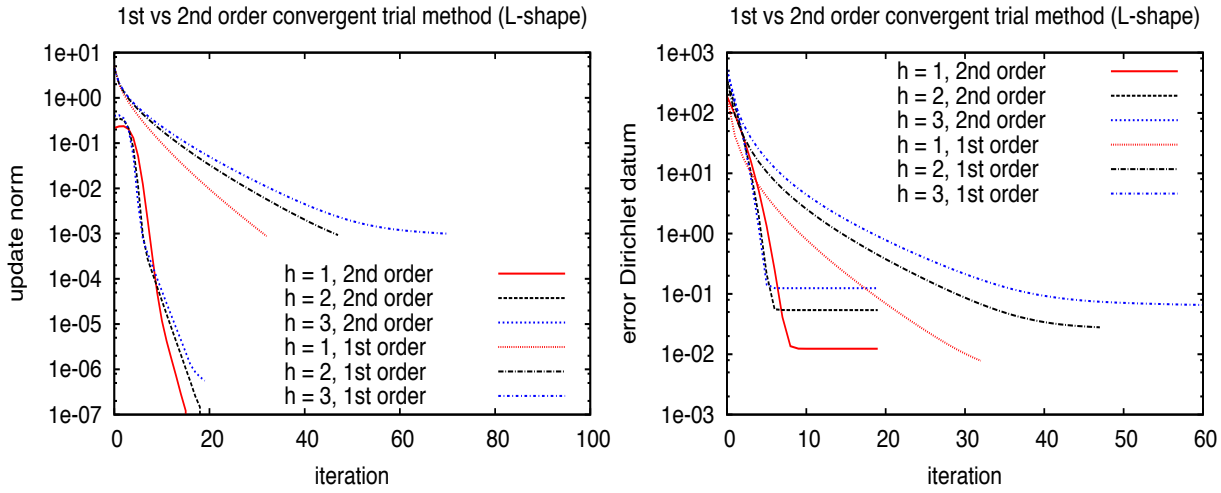

Figure 5.6: Histories of the norm of the update (left) and of the mismatch of the desired Dirichlet datum (right) in case of the first example.

determination is cheap compared with the assembling of the linear system (4.6) of equations which has to be performed once per iteration step of both trial methods. In that sense, the speed-up of the second order convergent trial method is essentially proportional to the reduction of the number of iterations of the trial method.

All computations have been carried out on a single processor of a computing server with four Intel(R) Xeon(R) X5550 CPUs with a clock rate of 2.67 GHz and 48 GB of main memory. The algorithm needs about 40 seconds per iteration step. Hence, the free surface computation by the second order convergent trial method consumes about five minutes computing time in all.

5.2 Second example

For our second example, let the interior domain S be the U-shape

$$S = ([-0.5, 0.5] \times [-1.5, 1.5] \times [-1, 1]) \setminus ([-0.5, 0.5] \times [-0.5, 0.5]^2)$$

and consider Bernoulli's original free boundary problem. This means, we seek the free boundary Γ with associated solution $u = u(\Gamma)$ such that it holds

$$\begin{aligned} \Delta u &= 0 && \text{in } \Omega, \\ u &= 1 && \text{on } \Sigma, \\ -\frac{\partial u}{\partial \mathbf{n}} &= h, \quad u = 0 && \text{on } \Gamma. \end{aligned}$$

Likewise to the first example, the constant field h will vary according to $h \equiv 1, 2, 3$.

To resolve the free boundary sufficiently accurate, we need to use Fourier series of length 400 for the representation of each coordinate of the parametrization, that is, harmonic polynomials up to order 20 can be represented exactly. Hence, we have 1 200 design parameters in all. When using only Fourier series of length 100 in each coordinate like in the first example, we have not been able to

resolve the geometric details of the free boundary in case of $h = 3$, see also Figure 5.9. The increase of accuracy in the boundary representation requires also an increase in the level of resolution in the discretization of the boundary integral equation. Thus, on level 5, we have about 22 000 piecewise bilinear boundary elements to discretize the domain's surface. For the Galerkin scheme (3.3), we apply 1 600 spherical harmonics. These settings result in a computing time of about 5 minutes per iteration of the first or second order convergent trial method on the same computer as in the previous example.

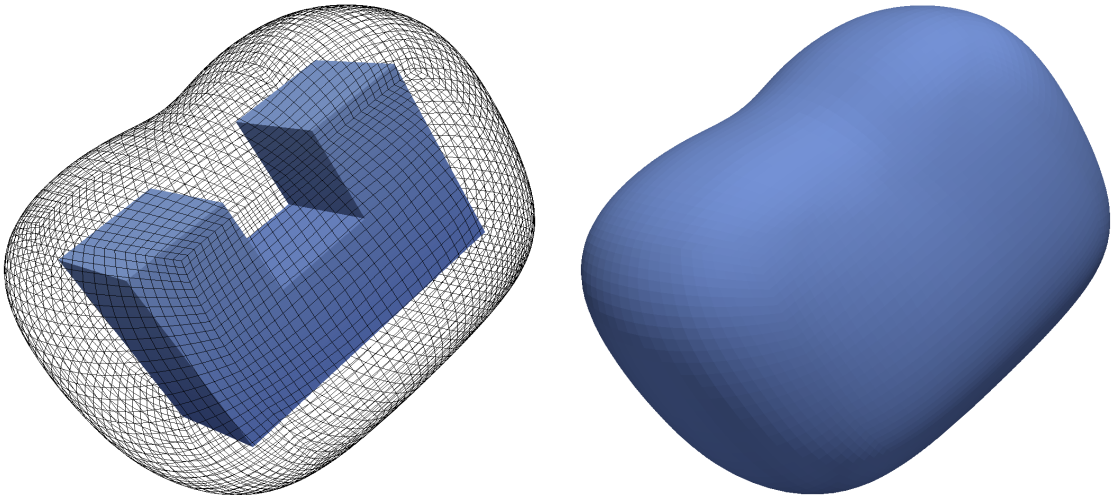

Figure 5.7: The free boundary of the second example in case of $h = 1$.

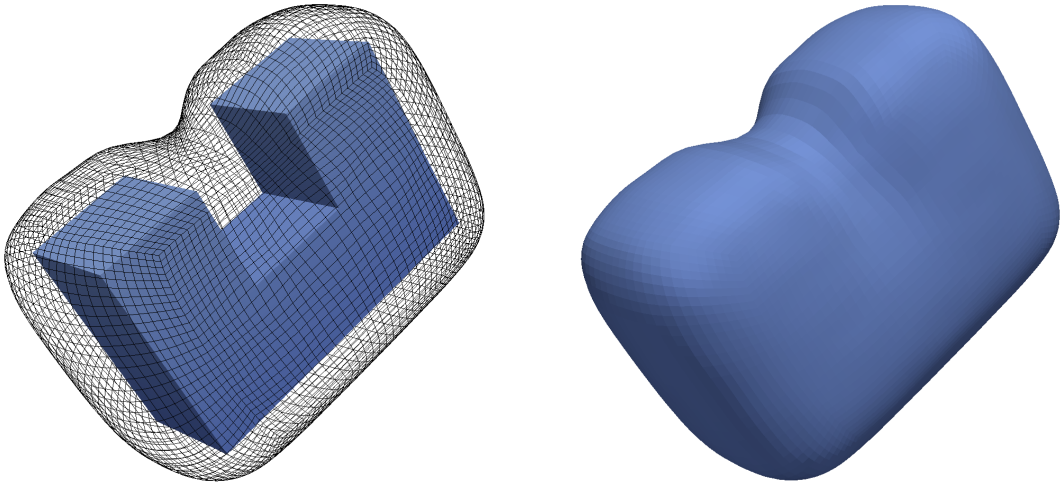

Figure 5.8: The free boundary of the second example in case of $h = 2$.

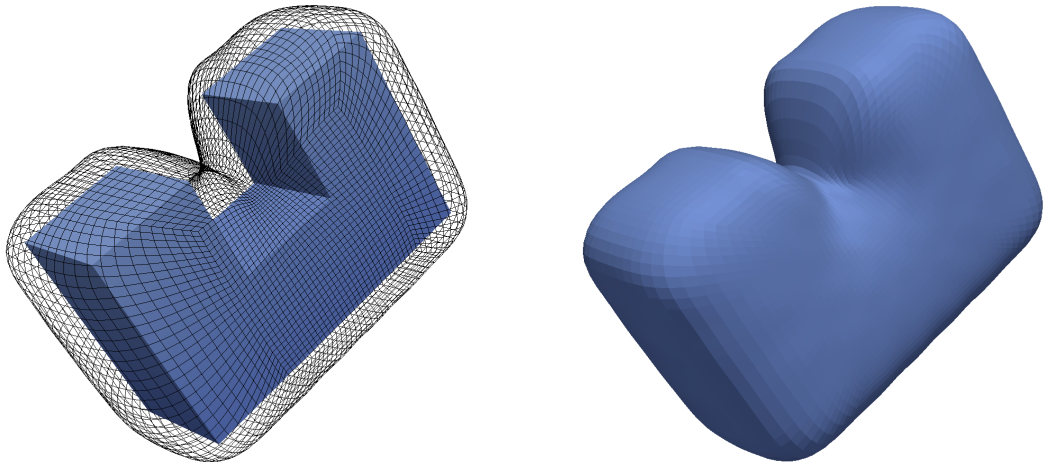

Figure 5.9: The free boundary of the second example in case of $h = 3$.

The results of our simulation are found in Figures 5.7–5.9. The mesh quality was always very good during the iteration steps of the first and second order convergent trial method such that there was again no need for a remeshing. Also as before, the second order convergent trial method converges much faster than the first order convergent trial method, compare Figure 5.10 where the histories of the norm of the update and the mismatch to the desired Dirichlet datum are plotted. We observe that the second order convergent trial method requires only about 5 iterations to have updates whose norms are always less than 10^{-3}. Compared with this, the first order convergent trial method requires about 10 times as much iterations. Hence, the use of the second order convergent trial method results in a speed-up by a factor of at least ten, which means less than 1/2 hour computing time versus more than 10 hours computing time.

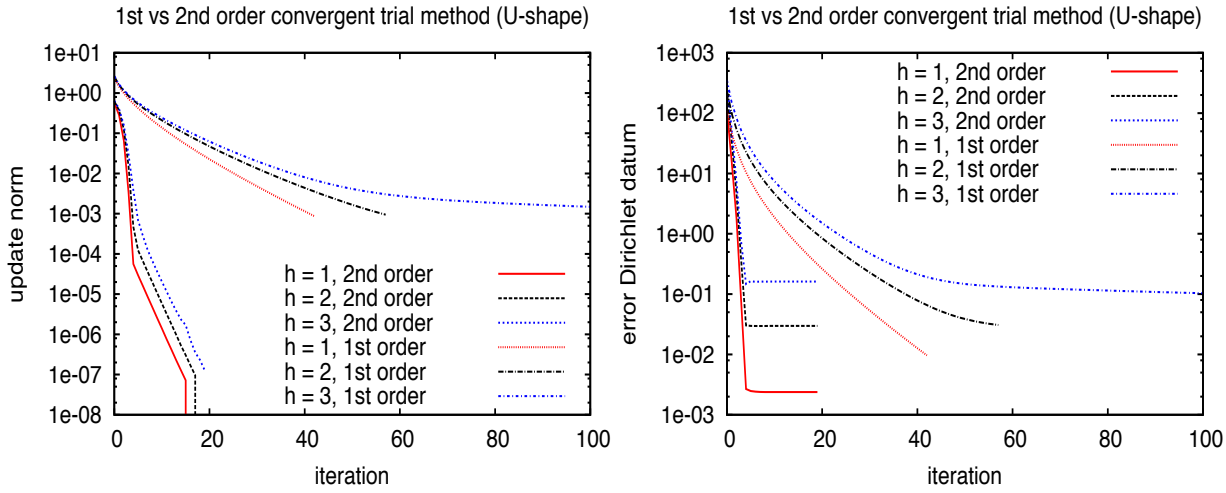

Figure 5.10: Histories of the norm of the update (left) and of the mismatch of the desired Dirichlet datum (right) in case of the second example.

6 Conclusion

In this article, we presented a second order convergent trial method for the solution of free boundary problems. The method coincides with the Newton method if the prescribed Neumann data are constant. Otherwise, it coincides with an inexact Newton method. The method has been introduced in [16] in case of starlike domains in two spatial dimensions and boundary updates in the radial direction. Here, we provided its realization for arbitrary domains in three spatial dimensions and boundary updates in the normal direction. Numerical experiments validated the feasibility and the second order convergence of this trial method.

Acknowledgments

This research was supported by the Swiss National Science Foundation through the project "Derivative free methods in shape optimization" (grant no. 200021_137668).

References

[1] A. Acker. How to approximate the solutions of certain free boundary problems for the Laplace equation by using the contraction principle. *Z. Angew. Math. Phys.*, 32:22–33, 1981.

[2] A. Acker. On the geometric form of Bernoulli configurations. *Math. Meth. Appl. Sci.*, 10:1–14, 1988.

[3] H.W. Alt and L.A. Caffarelli. Existence and regularity for a minimum problem with free boundary. *J. reine angew. Math.*, 325:105–144, 1981.

[4] F. Bouchon, S. Clain, and R. Touzani. Numerical solution of the free boundary Bernoulli problem using a level set formulation. *Comput. Methods Appl. Mech. Engrg.*, 194:3934–3948, 2005.

[5] F. Bouchon, S. Clain, and R. Touzani. A perturbation method for the numerical solution of the Bernoulli problem. *J. Comput. Math.*, 26:23–36, 2008.

[6] W. Dahmen, H. Harbrecht, and R. Schneider. Compression techniques for boundary integral equations. Asymptotically optimal complexity estimates. *SIAM J. Numer. Anal.*, 43:2251–2271, 2006.

[7] W. Dahmen and A. Kunoth. Multilevel preconditioning. *Numer. Math.*, 63:315–344, 1992.

[8] M. Delfour and J.-P. Zolesio. *Shapes and Geometries*. Society for Industrial and Applied Mathematics (SIAM), Philadelphia, PA, 2001.

[9] K. Eppler and H. Harbrecht. On a Kohn-Vogelius like formulation of free boundary problems. *Comput. Optim. Appl.*, 52:69–85, 2012.

[10] K. Eppler and H. Harbrecht. Tracking Neumann data for stationary free boundary problems. *SIAM J. Control Optim.*, 48(5):2901–2916, 2009.

[11] K. Eppler and H. Harbrecht. Shape optimization for free boundary problems. Analysis and numerics. In G. Leugering et al., editors, *Constrained Optimization and Optimal Control for Partial Differential Equations*, vol. 160 of Internat. Ser. Numer. Math., pp. 277–288, Birkhäuser, Basel, 2012.

[12] M. Flucher and M. Rumpf. Bernoulli's free-boundary problem, qualitative theory and numerical approximation. *J. reine angew. Math.*, 486:165–204, 1997.

[13] C. Geiger and C. Kanzow. *Theorie und Numerik restringierter Optimierungsaufgaben*. Springer, Berlin-Heidelberg, 2002.

[14] W. Hackbusch. *Integralgleichungen*. B.G. Teubner, Stuttgart, 1989.

[15] H. Harbrecht. A Newton method for Bernoulli's free boundary problem in three dimensions. *Computing*, 82:11–30, 2008.

[16] H. Harbrecht and G. Mitrou. Improved trial methods for a class of generalized Bernoulli problems. *J. Math. Anal. Appl.*, 420(1):177–194, 2014.

[17] H. Harbrecht and R. Schneider. Wavelet Galerkin schemes for boundary integral equations. Implementation and quadrature. *SIAM J. Sci. Comput.*, 27:1347–1370, 2006.

[18] H. Harbrecht and J. Tausch. On the numerical solution of a shape optimization problem for the heat equation. *SIAM J. Sci. Comput.*, 35(1):A104–A121, 2013.

[19] J. Haslinger, K. Ito, T. Kozubek, K. Kunisch, and G. Peichl. On the shape derivative for problems of Bernoulli type. *Interfaces Free Bound.*, 11:317–330, 2009.

[20] J. Haslinger, T. Kozubek, K. Kunisch, and G. Peichl. Shape optimization and fictitious domain approach for solving free boundary problems of Bernoulli type. *Comput. Optim. Appl.*, 26:231–251, 2003.

[21] J. Haslinger, T. Kozubek, K. Kunisch, and G. Peichl. An embedding domain approach for a class of 2-d shape optimization problems: mathematical analysis. *J. Math. Anal. Appl.*, 290:665–685, 2004.

[22] J. Haslinger and R.A.E. Mäkinen. *Introduction to Shape Optimization. Theory, Approximation, and Computation.* Society for Industrial and Applied Mathematics (SIAM), Philadelphia, PA, 2003.

[23] L. Hörmander. *The Analysis of Linear Partial Differential Operators.* Springer, New York, 1983–85.

[24] K. Ito, K. Kunisch, and G. Peichl. Variational approach to shape derivatives for a class of Bernoulli problems. *J. Math. Anal. Appl.*, 314:126–149, 2006.

[25] R. Kress. *Linear Integral Equations*. Springer, Berlin-Heidelberg, 1989.

[26] C.M. Kuster, P.A. Gremaud, and R. Touzani. Fast numerical methods for Bernoulli free boundary problems. *SIAM J. Sci. Comput.*, 29:622–634, 2007.

[27] P.A. Sackinger, P.R. Schunk, and R.R. Rao. A Newton-Raphson pseudo-solid domain mapping technique for free and moving boundary problems. A finite element implementation. *J. Comput. Phys.*, 125:83–103, 1996.

[28] F. Murat and J. Simon. Étude de problèmes d'optimal design. In *Optimization Techniques, Modeling and Optimization in the Service of Man*, edited by J. Céa, Lect. Notes Comput. Sci. 41, pp. 54–62, Springer, Berlin, 1976.

[29] O. Pironneau. *Optimal Shape Design for Elliptic Systems*. Springer, New York, 1983.

[30] Y. Saad and M.H. Schultz. GMRES: A generalized minimal residual algorithm for solving nonsymmetric linear systems. *SIAM J. Sci. and Stat. Comput.*, 7:856–869, 1986.

[31] J. Simon. Differentiation with respect to the domain in boundary value problems. *Numer. Funct. Anal. Optim.*, 2:649–687, 1980.

[32] J. Sokolowski and J.-P. Zolesio. *Introduction to Shape Optimization*. Springer, Berlin, 1992.

[33] O. Steinbach. *Numerical Approximation Methods for Elliptic Boundary Value Problems. Finite and Boundary Elements.* Springer, New York, 2008.

[34] D.E. Tepper. On a free boundary value problem, the starlike case. *SIAM J. Math. Anal.*, 6:503–505, 1975.

[35] T. Tiihonen. Shape optimization and trial methods for free-boundary problems. *RAIRO Model. Math. Anal. Numér.*, 31(7):805–825, 1997.

[36] T. Tiihonen and J. Järvinen. On fixed point (trial) methods for free boundary problems. In S.N. Antontsev et al., editors, *Free Boundary Problems in Continuum Mechanics (Novosibirsk, 1991)*, vol. 106 of Internat. Ser. Numer. Math., pp. 339–350, Birkhäuser, Basel, 1992.

[37] J.I. Toivanen, J. Haslinger, and R.A.E. Mäkinen. Shape optimization of systems governed by Bernoulli free boundary problems. *Comput. Methods Appl. Mech. Engrg.*, 197:3803–3815, 2008.

[38] J.-P. Zolesio. Numerical algorithms and existence result for a Bernoulli-like steady free boundary problem. *Large Scale Systems*, 6:263–278, 1984.

LATEST PREPRINTS

No.	Author: *Title*
2014-01	**Helmut Harbrecht, Michael Peters, Markus Siebenmorgen** *Efficient Approximation of Random Fields for Numerical Applications*
2014-02	**Ali Hyder, Luca Martinazzi** *Conformal Metrics on R^{2m} with Constant Q-Curvature, Prescribed Volume and Asymptotic Behavior*
2014-03	**Jürgen Dölz, Helmut Harbrecht, and Michael Peters** *H-Matrix Accelerated Second Moment Analysis for Potentials with Rough Correlation*
2014-04	**Tianling Jin, Ali Maalaoui, Luca Martinazzi, Jingang Xiong** *Existence and Asymptotics for Solutions of a Non-Local Q-Curvature Equation in Dimension Three*
2014-05	**Marcus J. Grote, Michaela Mehlin, Teodora Mitkova** *Runge-Kutta Based Explicit Local Time-Stepping Methods for Wave Propagation*
2014-06	**Hanspeter Kraft, Andriy Regeta** *Automorphisms of the Lie Algebra of Vector Fields on Affine n-Space*
2014-07	**Jérémy Blanc, Alberto Calabri** *On Degenerations of Plane Cremona Transformations*
2014-08	**Helmut Harbrecht, Michael Peters, Markus Siebenmorgen** *Numerical Solution of Elliptic Diffusion Problems on Random Domains*
2014-09	**H. Harbrecht, W.L. Wendland, and N. Zorii** *Rapid Solution of Minimal Riesz Energy Problems*
2014-10	**Julien Diaz, Marcus J. Grote** *Multi-Level Explicit Local Time-Stepping Methods for Second-Order Wave Equations*
2014-11	**J. Dölz, H. Harbrecht, Ch. Schwab** *Covariance Regularity and H-Matrix Approximation for Rough Random Fields*
2014-12	**Giovanni Alberti, Gianluca Crippa, Anna L. Mazzucato** *Exponential Self-Similar Mixing and Loss of Regularity for Continuity Equations*

LATEST PREPRINTS

No. **Author:** *Title*

2014-13 **M. Dambrine, H. Harbrecht, B. Puig**
Computing Quantities of Interest for Random Domains with Second Order Shape Sensitivity Analysis

2014-14 **Monica Bugeanu, Helmut Harbrecht**
A Second Order Convergent Trial Method for free Boundary Problems in Three Dimensions